Proceedings of the
4th JSME-KSME Thermal Engineering Conference
October 1-6, 2000, Kobe, Japan

F208

THE FLOW OVER AN INCLINED SMALL FENCE IN A TURBULENT BOUNDARY LAYER

Yuji Okita*,

Kyozo Ayukawa**, **Katsutaka Nakamura***, **Masashi Ichimiya***** and **Yoshiyuki Nakase*****

*Anan College of Technology, 265 Aoki, Minobayasi-cho, Anan, Tokushima, 774-0017 Japan

**Ehime University, 10-13 Dogohimata, Matsuyama, Ehime, 790-8577 Japan
***University of Tokushima, 2-1 Minamijyosanjima, Tokushima, 770-8506 Japan

ABSTRACT The purpose of this paper is to study in detail the flow over an inclined fence in a turbulent boundary layer, as basic research which issues from promoting heat transfer and the decrease of the pressure drop. The fence height h set in a turbulent boundary layer is 3 mm($u_\tau h/\nu = 75, u_\tau$: friction velocity, ν : kinematic viscosity) and setting angle of a fence is 20° in the main stream direction. The time-average velocity profiles in the downstream of the fence were measured by using a 3-hole pitot tube. We investigated velocity profiles by utilizing polar diagram, logarithmic velocity distributions and velocity defect law. Consequently, it was found that the spanwise velocity profiles are cross-over profiles. We clarified the relaxation process from stream-wise direction velocity. Further we investigated in detail the flow direction on the wall which shows the wall shear direction by the oil flow visualization.

Keywords : Turbulent Flow, Boundary Layer, Three-dimensional Flow, Separation, Relaxation Process

1. INTRODUCTION

There were much on the flow around a obstacle(1), and it has a wide application to the increase of heat transfer, the drag of a obstacle.

When we seek to promote heat transfer, it is important that not only the increase of the heat transfer but also the decrease of pressure drop. In general, we face the conflicting problem in which the roughness drag on the tube wall serves to promote the heat transfer for a exchanger tube, and causes a greater pressure drops. Recently, some inner spiral fin tubes with a long pitch fin and inclined ribrets on the wall have been used to overcome this problem(2). However, the flow mechanism in this inner spiral fin tubes has not been clarified to date.

When a three-dimensional boundary layer is generated in the downstream of the inclined two dimensional obstacle, it has been reported that the local friction drag coefficient or turbulent kinetic energy decreases in DNS(4)(5).

Therefore, the purpose of this paper is to study in detail the flow over an inclined fence in a turbulent boundary layer. We would like to show the relaxation process of the three-dimensional turbulent boundary layer downstream of the small fence by using a 3-hole pitot tube.

2. EXPERIMENTAL APPARATUS AND TECHNIQUES

Experiments were carried out in the open-circuit wind tunnel at the Anan College of Technology. The wind tunnel is 4.4 m in length, and 1/5 in contraction. The duct tube (300 mm × 200 mm) is connected at the outlet of the wind tunnel. The inlet flow was tripped by the tipping wire (ϕ 1.0 mm) set 220 mm away from the leading edge of the tunnel floor to ensure that the boundary layer is turbulent. The small fence was mounted on the test plate of the position 1.5 m away from the leading edge illustrated in figure 1. The fence set in a turbulent boundary layer is 3 mm in height, denoted h ($u_\tau h/\nu = 75, u_\tau$: friction velocity, ν : kinetic viscosity) and a fence is set on a angle of 20° with the main stream direction.

We used a 3-hole pitot tube to measure the time-average velocity profiles in the down-stream of the fence. The end of the pitot tube is flat shape of 0.5 mm in height and 2.9 mm in width and all opening heights

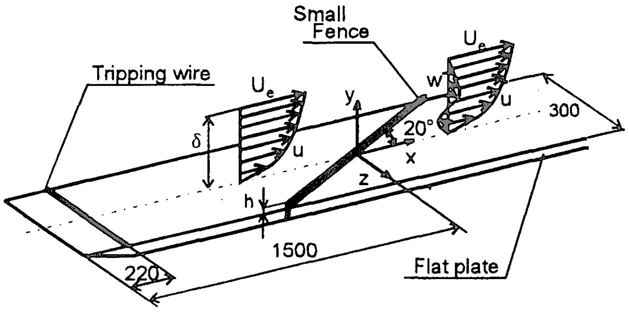

Fig. 1 Flow field and coordinate system

were 0.3 mm. The measurements of the time-average velocity profiles were carried out along the center line in spanwise direction. The unit Reynolds number U/ν was $6 \times 10^5 m^{-1}$.

A surface oil-flow technique was used to show the limiting streamline or skin friction line structure. The mixture used in this study was 100 cc of Linseed oil and 3 g of Oil paint(white).

3. EXPERIMENTAL RESULTS AND DISCUSSION

3.1 Wall static pressure distribution

The wall static pressures were measured in the region behind and in front of the small fence to investigate the pressure gradient in the stream-wise direction. The figure 2 shows the wall static pressure coefficient C_p normalized by the wall static pressure at the upstream reference point. The measured points are chosen along the line of z/h=-25, 0, +25 in spanwise direction. x_f is the stream-wise distance from the location at which the small fence is mounted at any spanwise location, that is,

$$x_f = x + z\tan 70^\circ \tag{1}$$

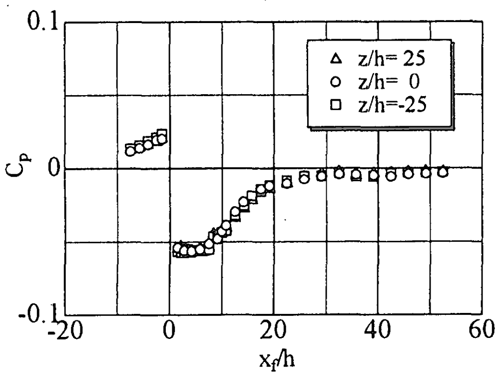

Fig. 2 Wall static pressure distribution

In the forward region of the fence, the wall static pressure has maximum value at just the forward point of the fence which is the stagnation point. On the other hand, the wall static pressure has the minimum value at just the behind point of the fence. This may be caused by flow separation over the fence. Towards downstream from this point, are formed the reverse pressure gradient which led to the pressure at the downstrem uniform flow. The agreement of the profiles of the different locations of z shows that wall static pressure profiles will be uniform along x-direction at any location of the small fence.

3.2 Mean velocity profiles

The figure 3 and figure 4 show the stream-wise velocity u and the spanwise velocity profiles w in the boundary layer measured by use of 3-hole pitot tube. The u and w are normalized by the main stream U_e. The profiles of u/U_e change largely at the locations of x/h=8.3, 15 where flow separat by the small fence. After that, the profile recovers to the profile of h=0 with increasing x/h. Further the profiles of w/U_e change profiles of the cross-over type in which there is an intermediate position where the cross-flow is in opposite directions at different levels in the boundary layer. The spanwise velocity has a negative value in the near wall, while it has a positive value in the higher position than fence height. The value in the x/h=8.3 which is just behind the small fence changes most, and the change becomes small with increasing x/h.

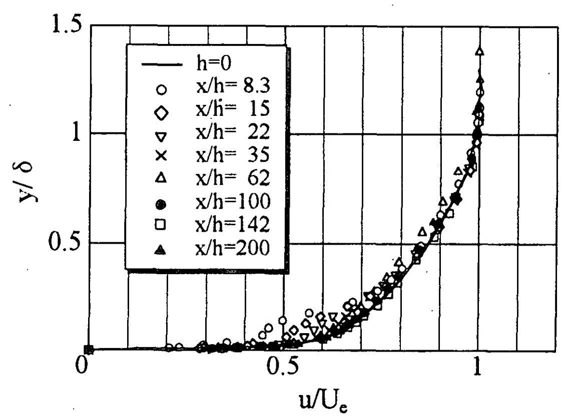

Fig. 3 Mean velocity profiles (x-direction)

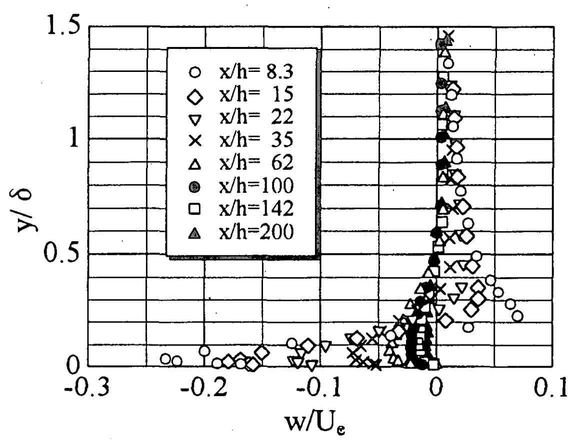

Fig. 4 Mean velocity profiles (z-direction)

Figure 5 shows the polar plots which indicate the relation between u/U_e and w/U_e. The dotted lines show the angle of the small fence. In this figure, since the values of w/U_e have positive or negative values, the polar plots shows interesting feature. The velocity angle near the wall is larger than the fence angle in x/h=8.3,15. These points may be located in the separation region, in which the flow velocity is slow, it may be suggested that the cross-flow caused in the separation region behind the small fence affected strongly the flow in this region. We would suggest that the cross-flow is a primary factor for increasing heat transfer in the inner spiral fin tubes.

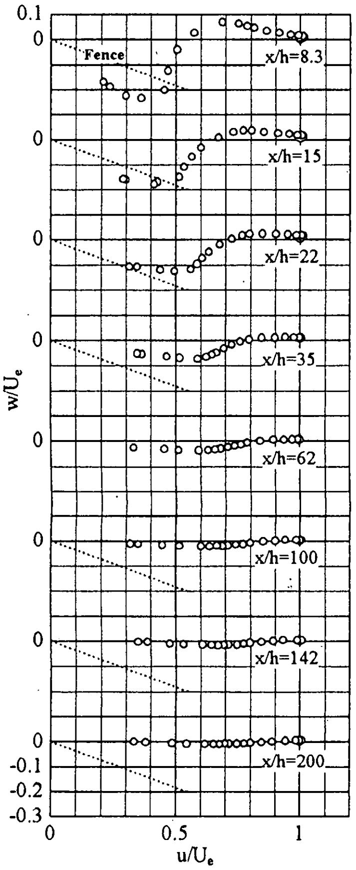

Fig. 5 Polar plots

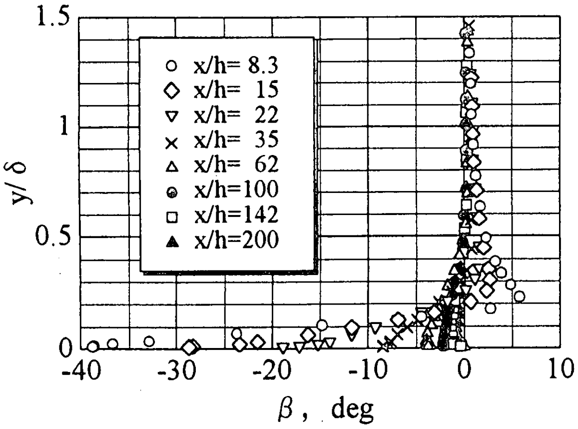

Fig. 6 Cross-flow angle profiles

Figure 6 shows cross-flow angle profiles β. As mentioned above, the velocity angle is large at near wall of x/h=8.3, 15. From this figure, the variations of the limiting angles at the wall calculated by Eq. (2) are indicated in figure 7.

$$\beta_0 = \lim_{y \to \infty} \tan^{-1}(w/u) \tag{2}$$

In this figure, it may be assumed that at the location x/h=22, where the velocity angle is equal to the fence angle, there is a reattachment point. Figure 8 shows the flow visualization picture on the wall, the white streamline angle is a similar to the result of figure 7.

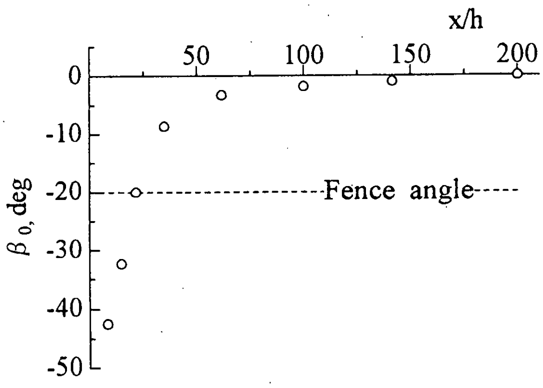

Fig. 7 Limiting streamline angle

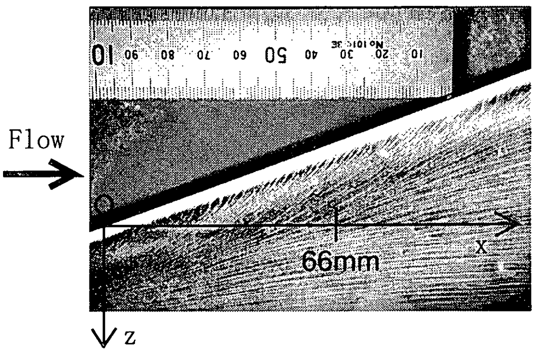

Fig. 8 Oil flow visualization on the wall

3.3 Local skin friction and logarithmic velocity distributions

Since the flow field in this study is considered as the three-dimensional perturbations of two-dimensional turbulent boundary layer, and, generally the direction of the main flow is similarly indicated as a two-dimensional flow, as indicated by Muller[6] and Yamashita[3]. Therefore, we treat similarly the values of x-direction as two-dimensional turbulent boundary layer.

First, figure 9 shows the variation of the local skin friction coefficient c_f estimated from the resultant mean velocity profile data using Clauser's technique. In addition, the solid line indicates the data from the local

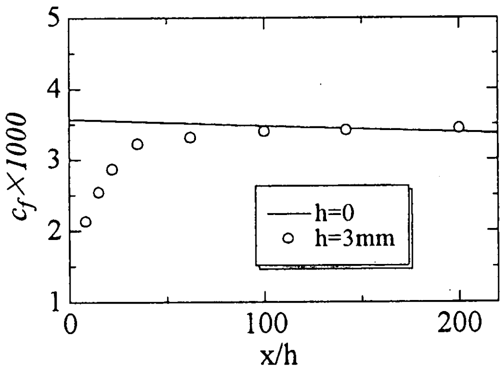

Fig. 9 Local skin friction coefficient

skin friction coefficient in the two-dimensional turbulent boundary layer (in the absence of the fence). The local skin friction coefficient increases rapidly in the region close to the small fence, the rate of increase decreases with the downstream distance. And both values show agreement at around x/h=100. Although the limiting wall angles β_0 are not equal to zero in this location, the rapid change declines at this location.

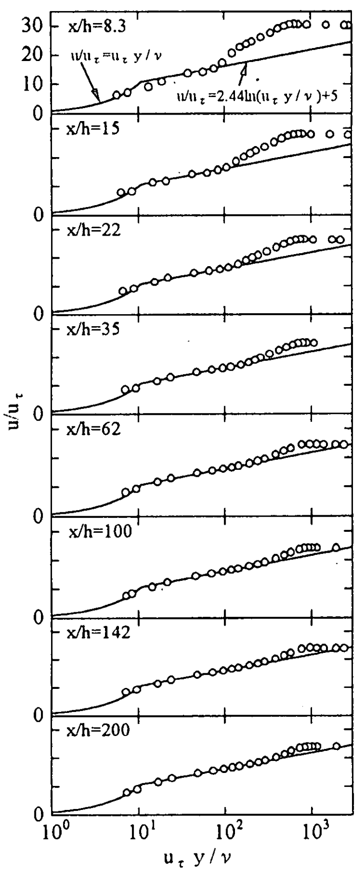

Fig. 10 Logarithmic velocity profiles

Figure 10, and 11 show the logarithmic velocity profiles and the velocity-detect law normalized by the local skin friction velocity estimated using the Clauser's technique. In the x/h=8.3 of figure 10, the region co-incidencing with the wall-law is narrow. This region increases with increasing x/h. In the velocity-defect law figure 11, though the disagreement with the wall-law is large in the region close to the small fence, the distributions agree with wall-law beyond x/h=100. This relaxation process will indicate a similar tendency. Therefore figure 12 shows the variation in the wake parameter $\Pi(=(1/\kappa)(\Delta u/u_\tau)$ κ:karman constant=0.41) estimated from figure 10. Figure 12 shows a similar tendency, which becomes constant at around x/h=100.

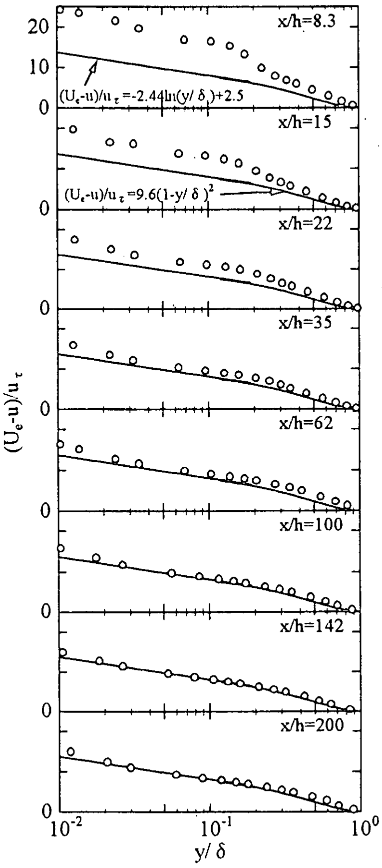

Fig. 11 Velocity-detect law

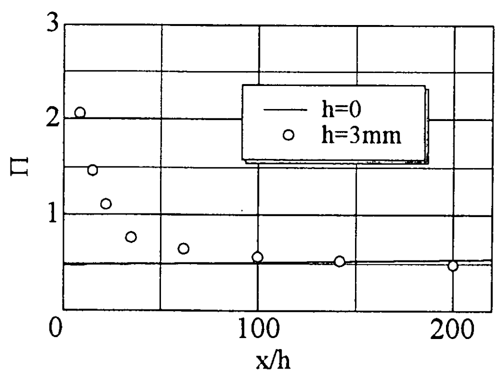

Fig. 12 Wake parameter

3.4 Integral thickness

Figurere 13 shows the variation in the displacement thickness δ^*, the momentum thickness θ and shape factor H. The displacement thickness is large in the region close to the small fence, and its value tends to decrease once with increasing x/h. On the other hand, the change of the momentum thickness is not large in comparison with the displacement thickness in the region close to the fence. After that, because of the both values increase with increasing x/h, shape factor indicates the condition which become constant at around x/h=100. From these results, it may be assumed that the three-dimensional turbulent boundary layer in this case recover to two-dimensional boundary layer at around x/h=100.

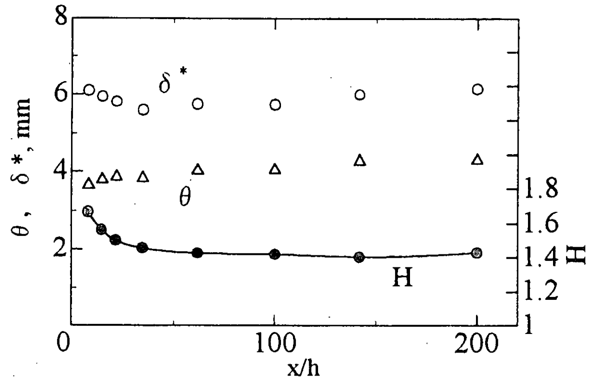

Fig. 13 Integral thickness and shape factor

4. CONCLUSION

The following conclusions were derived from the experimental results for the flow over was inclined small fence mounted in a turbulent boundary layer.

(1) The two-dimensional turbulent boundary layer changes the skewed three-dimensional turbulent-boundary layer which exhibits cross-over profiles in which there is an intermediate position where the cross-flow changes its directions at different levels in the boundary layer.

(2) The direction of the limiting flow angle indicates the values larger than 20° behind and close to the small fence. It may be suggested that a cross-flow causes in the separate region behind the fence, and it may be assumed that reattachment point is the location in about x/h=22.

(3) The measured values in x-direction coincide with two-dimensional case beyond x/h=100, for instance, the shape factor becomes constant beyond about x/h=100. On the other hand, long distance may be required in this case till the spanwise velocity becomes zero.

5. REFERENCES

(1) Good, M.C. and Joubert, P.N.,. The form drag of two-dimensional bluff-plates immersed in turbulent boundary layers, *J.Fluid Mech.*, **31** (1968), 547-582.

(2) Itou, M. and Kimura, H., Trans. Japan Society of Mechanical Engineers, Ser. B **51**-469, (1985), 118-126.

(3) Yamashita, S. et al., Experiments on a Three-Dimensional Turbulent Boundary Layer over a Ridge (1st Report, Mean Flow Field at Yaw Angle 30°), Trans. Japan Society of Mechanical Engineers, Ser. B **54**-500, (1988), 823-832.

(4) Bradshaw, P. and Pontikos, N.N., Measurments in the turbulent boundary layer on an 'infinite' swept wing, *J.Fluid Mech.*, **159** (1985), 105-130

(5) Moin, P. et al., Direct numerical simulation of a three-dimensional turbulent boundary layer, *Phys.Fluids*, A2-10(1990), 1846-1853.

(6) Muller, U.R., Measurments of the Reynolds stresses and the mean-flow field in a three-dimensional pressure-driven boundary layer, *J.Fluid Mech.*, **119** (1982), 121-153.